

## USIMAGTOOL: AN OPEN SOURCE FREEWARE SOFTWARE FOR ULTRASOUND IMAGING AND ELASTOGRAPHY

Rubén Cárdenes-Almeida<sup>1</sup>, Antonio Tristán-Vega<sup>1</sup>, Gonzalo Vegas-Sánchez-Ferrero<sup>1</sup>, Santiago Aja-Fernández<sup>1</sup>, Verónica García-Pérez<sup>1</sup>, Emma Muñoz-Moreno<sup>1</sup>, Rodrigo de Luis-García<sup>1</sup>, Javier González-Fernández<sup>2</sup>, Darío Sosa-Cabrera<sup>2</sup>, Karl Krissian<sup>2</sup>, Suzanne Kieffer<sup>3</sup>

<sup>1</sup> LPI, University of Valladolid, Spain

<sup>2</sup> CTM, University of Las Palmas de Gran Canaria

<sup>3</sup> TELE Laboratory, Université catholique de Louvain, Louvain-la-Neuve, Belgium

### ABSTRACT

*UsimagTool* will prepare specific software for the physician to change parameters for filtering and visualization in Ultrasound Medical Imaging in general and in Elastography in particular, being the first software tool for researchers and physicians to compute elastography with integrated algorithms and modular coding capabilities. It will be ready to implement in different ecographic systems. *UsimagTool* is based on C++, and VTK/ITK functions through a hidden layer, which means that participants may import their own functions and/or use the VTK/ITK functions.

### KEYWORDS

Software – Medical Imaging – Ultrasound – Elastography

### 1. INTRODUCTION

The extraordinary growth experimented by the medical image processing field in the last years, has motivated the development of many algorithms and software packages for image processing. One of the most important set of algorithms for image processing can be found in the Insight Toolkit (ITK) [1] open source libraries for segmentation and registration of multidimensional data. At the same time, several software packages for medical image visualization and analysis have been developed using ITK and the visualization toolkit (VTK) [2] libraries. There are also some efforts to develop software that could be easy to modify by other researchers, for example the Medical Imaging Interaction Toolkit (MITK) [3], is intended to fill the gap between algorithms and the final user, providing interaction capabilities to construct clinical applications.

Therefore, many software packages for visualization and analysis of medical data are available for the research community. Among them we can find commercial and non commercial packages. Usually, the former ones are focused on specific applications or just on visualization being more robust and stable, whereas the latter ones often offer more features to the end user, and they are usually available as open source projects. Some of the non commercial packages equipped with graphic user interface (GUI), are 3D Slicer [4, 5], Julius [6], Osirix [7], ITK-SNAP [8], Medical Studio [9], MedInria [10], Amide [11] and FusionViewer [12], to cite some of them. Other important commercial software packages are Analyze [13], Amira [14] and 3D Doctor [15].

The requirements that we look for in a medical imaging software package for researchers can be summarized in the following list:

- Open source code: to be able for everyone to modify and reuse the source code.
- Efficiency, robust and fast: using a standard object oriented language such as C++.
- Modularity and flexibility for developers: in order to change or add functionalities as fast as possible.
- Multi-platform: able to run in many Operating systems to be useful for more people.
- Usability: provided with an easy to use GUI to interact as easy as possible with the end user.
- Documentation: it is important to have a well documented web site as well as a complete user and developer manuals or tutorials.

Among the non commercial packages mentioned before, Amide and FusionViewer do not accomplish all these features because they are not specially designed for developers, and they are not well documented for that, Osirix is only available for Mac OS, MedInria is not open source, Medical Studio is in an early stage of development, and only ITK-SNAP, Slicer and Julius accomplish almost all of the features mentioned, but their structure is relatively complex compared with the architecture of *UsimagTool*, thus they do not offer a flexible architecture for researchers. We propose here a package that fulfills all these requirements and at the same time is equipped with a set of algorithms for ultrasound (US) image processing, which makes this package one of the few software packages developed for US image processing.

### 2. INTERFACE

This section describes the new interface developed for *UsimagTool*, as well as the new ways for the interaction between the user and the tool.

#### 2.1. General Structure

The general view of the *UsimagTool* interface appears in Figure 1, where it can be seen that the interface is divided into two main parts: the processing and configuration part and the visualization part. The first one is on the left-hand side of the application window, and it is divided into three subparts:

1. **Type of Processing.** It is a menu for selecting the type of processing (see Figure 2). When a type of processing is selected, multiple filters and algorithms related to the selected type appear in the options panel. These options are thought to be reconfigurable.

2. **Options Panel.** This panel presents the most usual algorithms for each processing type.
3. **Configuration Panel.** Here all the parameters of each filter can be selected, as well as the input/output origin or visualization destinations.

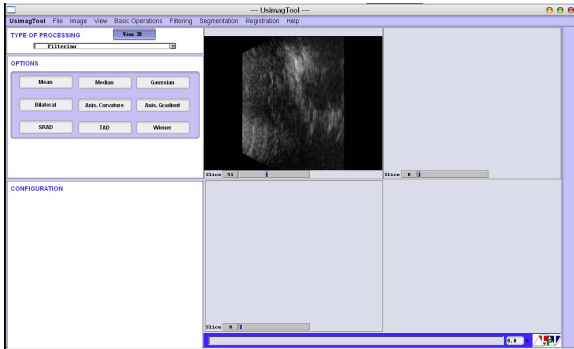


Figure 1: General view of the UsimagTool graphic user interface

The visualization part is on the right-hand side of the application window. There are multiple visualization options available: 3D Surface Rendering, Orthogonal visualization and Split visualization. Each visualization mode can be selected pressing the corresponding button.

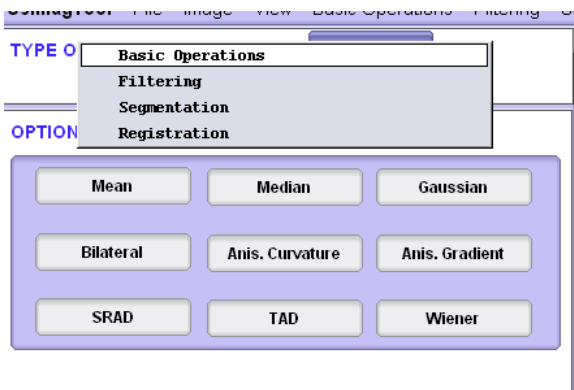


Figure 2: Type Processing menu

## 2.2. Menus

In order to provide an easy and fast access to all the basic operations as well as all the image processing algorithms available, UsimagTool is organized using different menus for different group of operations. Figure 3 shows the area of the interface where the menus are placed. Next, we briefly describe the structure and options of the different menus:

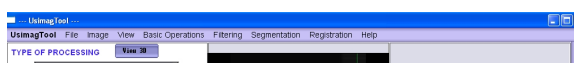


Figure 3: Detail of the UsimagTool interface showing the different menus.

ture and options of the different menus:

1. **UsimagTool:** This menu allows to access to three general options of the program:

- **About UsimagTool:** This operation is intended to show information about the program release and versions. It has not been implemented yet.
- **Preferences:** Using this option, the user can access the general setting of the program, which will appear in the *Configuration Area*.
- **Quit UsimagTool:** This option exits the program.

2. **File:** This menu gives access to file input and output operations:

- **Open:** This option opens a selection window for choosing an image or volume file in several file formats: metaheader, raw data (in another menu item), voluson, DICOM, JPEG, PNG, TIFF.
- **Open Raw:** This operation opens a selection window for raw data, and also another window for the introduction of the necessary parameters (see Figure 4).

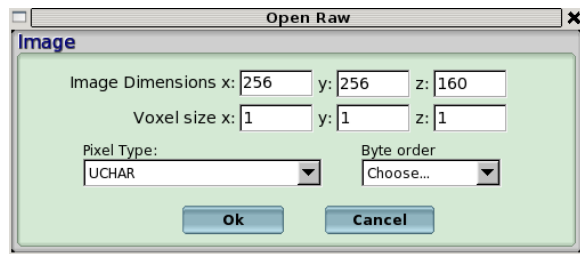


Figure 4: Parameter window for the "Open Raw" operation.

- **Save:** Using this option, the current image in the selected viewer is saved. A window appears where the file name needs to be chosen. Metaheader, voluson, DICOM, JPEG, PNG and TIFF are supported.
- **Save as:** This option is not yet implemented.

3. **Image:** This menu has been designed for easy access to some useful operations in the visualization of the images and volumes. Currently, these options are not accessible using this menu and can only be employed using keyboard buttons.

4. **View:** In this menu, three different visualization options can be selected:

- **Split:** Four viewers allow the independent visualization of four 2D images. This is the default option.
- **Orthogonal:** For a 3D volume, three orthogonal views are shown: sagittal, axial and coronal.
- **Surface Rendering:** For a 3D surface polydata file in VTK, this option shows the surface in 3D. Zoom in, zoom out and 3D rotation can be then performed.

5. **Basic Operations:** This menu provides access to some basic image processing operations, such as addition, difference, multiplication (these three operations need two input images), erosion, dilation, gradient, rescaling, re-labeling, absolute difference and inverse image. Some of these operations need the configuration of some parameters. If this is the case, a configuration window will appear to this end.

6. *Filtering*: Within this menu, different filtering algorithms are placed, from the most basic mean, median or Gaussian filtering to the most advanced bilateral or Wiener filtering. Besides, two more groups of filtering algorithms are implemented: Edge detection algorithms (zero-crossing edge detector and Canny detector), and anisotropic filtering (with five different variants).
7. *Segmentation*: This menu offers three different segmentation algorithms. First, a basic thresholding algorithm is proposed. Second, a level set segmentation algorithm has been implemented, and finally a supervised kNN algorithm can be employed. All three methods need different parameters to be tuned and therefore open a configuration panel in the configuration area.
8. *Registration*: Two registration algorithms are to be implemented in this menu. First, a demons registration algorithm (which opens a configuration panel). Second, a TPS (Thin Plate Splines), which is not implemented yet.
9. *Help*: This menu provides access to different help options, which are not implemented yet.

### 2.3. Configuration Area

As roughly indicated in Section 2.1, the left side of the application window is dedicated to configuration purposes. When a general type of processing is selected in the top part, the most common processing operations belonging to that type appear in the Options Panel, as was explained before and showed in Figure 2. Then, when a particular operation is chosen by pressing the corresponding button or by selecting it in the different operation menus explained in Section 2.2, the different configuration options of this particular processing operation will appear in the Configuration Panel. Besides these options, which depend on the particular choice of the operation, the user can also select which viewer will be selected as an input for the processing algorithm<sup>1</sup>, and which viewer will be selected for the visualization of the algorithm output.

### 2.4. Visualization Area

The right part of the application window is the Visualization Area. *UsimagTool* provides three main visualization modes: Split Mode, Orthogonal Mode (not implemented yet) and 3D Rendering Mode. Depending on the visualization mode, which can be chosen in the right end of the application window, the Visualization Area changes its appearance.

#### 2.4.1. Split Mode

Once the data is loaded, the image appears in one of four main viewers of the interface. These windows always show 2D images, but they are capable of representing the different orthogonal cuts of a volume (pressing the buttons 0,1,2 when the cursor is on them). Furthermore, there is a *slider* at the bottom of every viewer that allows to change the cut showed when the data is a volume. The visualization of the processed information can be done in any of the four main viewers.

The destination viewer for the output of every filter is controlled in the Configuration Panel.

There are different visualization operations that are available for each visualization window, and are accessible pressing the corresponding button as explained in Table 1.

<sup>1</sup>For certain types of algorithms, several images or volumes must be selected as inputs.

0	See cuts in the x axis
1	See cuts in the y axis
2	See cuts in the z axis (by default)
i ,	See the following cut
j ,	See the previous cut
r	Reset all the options
h	Help (this summary)
x	Flip x axis
y	Flip y axis
z	Flip z axis
q w	Diminishes, increases the top limit of the window in intensity
e	alternates the values of the top limit windows in intensity between <i>clipping</i> and <i>setting-to-black</i>
a s	Diminishes, increases the lower limit of the window in intensity
d	Alternates the values of the lower limit windows in intensity between <i>clipping</i> and <i>setting-to-black</i>
+ =	Zoom-in a factor 2
- _	Zoom-out a factor 2
i m j k	Moves the image in the directions up, down, left, and right.
t	Transposes the axis of the cut showed
A	See axis labels: P=posterior, L=left, S=superior
C	See crosses where the cursor was last clicked
I	See image values where the cursor was last clicked
T	Show or hide the clicked points
P	Change the coordinates between index and physical units
D	See image details superposed
O	See a superposed color
p	Save to a file the clicked points
l	Change the the screen data showing way Ways change cyclically in the following views: Intensity Inverse Log Derivative respect to x Derivative respect to y Derivative respect to z Mix with the previous and following cut MIP

Table 1: Available options in the visualization windows

#### 2.4.2. Orthogonal Mode

This visualization mode is not implemented yet.

#### 2.4.3. 3D Rendering Mode

This mode allows the visualization of a 3D surface. When it is selected, the corresponding data file can be loaded, and then the 3D surface is rendered. Zoom and rotation can be applied in this visualization mode (see Figure 5).

### 2.5. Points management

We have included a module for points management, useful in many situations such as landmark based registration, initialization of region growing of level set algorithms and other supervised algorithms like the k nearest neighbors algorithm. The functionalities included in this module are:

- Add point.

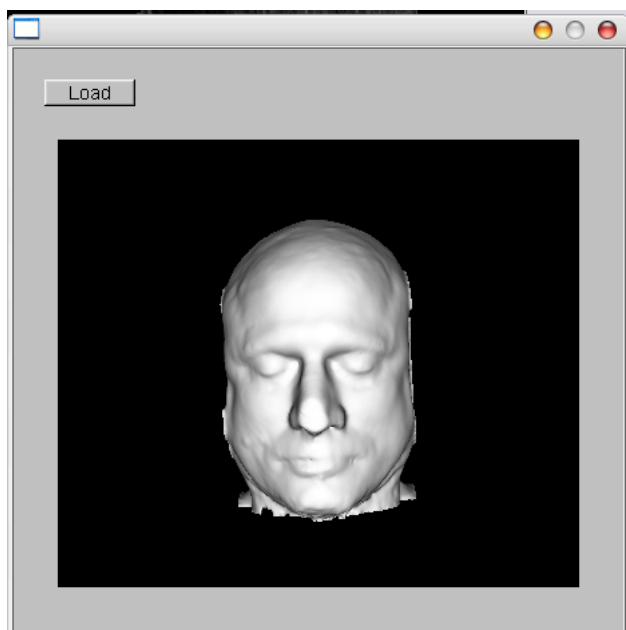


Figure 5: Rendering volume window

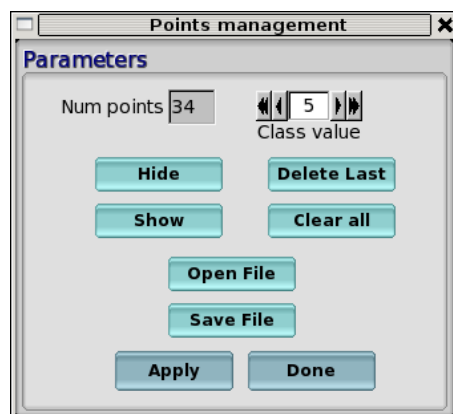


Figure 6: Points management module

- Open an existing points file.
- Save the points selected to a file.
- Clear all points.
- Delete last point.
- Change the id of the points to add.
- Show and hide the points in the viewer.
- List number of points selected.

## 2.6. Preliminary integration of an intuitive device for navigation

Successful image manipulation requires an intuitive user interaction. We propose an original navigation device which allows the user to interact with and manipulate items on screen through the use of accelerometers and optical sensors. A wireless one-handed remote control is presented instead of the traditional cursor-based navigation of current medical consoles.



Figure 7: Wii remote control device

Nintendo's Wii Remote has been used as a low-cost prototype, see fig 7. It has the ability to sense acceleration along three axes through the use of an Analog Devices ADXL330 accelerometer. The Wii Remote also features an infrared (IR) optical sensor, allowing it to determine where the Wii Remote is pointing at if an external infrared bar is used. It includes eleven buttons for user-interaction. It communicates wirelessly with the PC via short-range (10 meters) Bluetooth radio.

A customized 'wiiuse' library [16] has been used. It is completely written in C and meant to be portable between Linux and Windows platforms. It has been preliminary tested on Linux hosts, making use of BlueZ bluetooth drivers that permit communication with Bluetooth HID-capable devices. It is capable of capturing button press events, motion sensing (tilt), and will include support for IR pointing in the future.

User interaction has been prototyped as follows: pitch and roll angles control Y and Z navigation, respectively. Zoom level is controlled by means of the Wiimote's cursor pad. Blue Light Emitting Diodes (LED) show different user modes or the active window.

## 3. WORKPACKAGES

### 3.1. Basic Operations

In order to support pre and/or post processing of the data images, some basic operations are included in this tool. They include gradient magnitude computation, addition and multiplication of images, relabeling of segmented images, connected components labeling, inversion of images, Canny edge detection filtering, and binary morphological operations (erosion, dilation, opening and closing). All of them are implemented using standard filters of ITK.

### 3.2. Segmentation

We include in *UsimagTool* some classic algorithms such as basic thresholding and level sets previously implemented in the ITK. The main algorithms implemented in our tool, that are not part of the official ITK release are the k nearest neighbors segmentation and a segmentation method based on a MRF model.

### 3.2.1. *K nearest neighbors (kNN)*

We have included the *k* nearest neighbors segmentation (kNN) algorithm in *UsimagTool*. The kNN algorithm is a supervised non parametric technique used for years mostly to segment Magnetic Resonance Images (MRI). Its main drawback was its computational complexity to find the neighbors in the feature space, but this issue was drastically reduced by using lookup tables based on high order Voronoi Diagrams, as proposed in [17] and [18]. The implementation used here is based on those publications, and the algorithm is coded in ITK, and it is also publicly available in [19]. As this is a supervised method, the user needs to initialize or to train the classifier, by clicking several pixels in the image, and assigning to each pixel the class it should belong to. For this reason we can use the point management module explained above for this training step. We have designed a wizard (see Figure 8) to guide a non expert user to use this algorithm. It consists of three windows: first window to choose parameters and input/output, the second window to choose between load existing points or train the classifier and the third one for landmark manipulation.

In Figure 9 we show the result of this algorithm applied to a MRI of a human brain.

### 3.2.2. *Kidney segmentation*

This is a semiautomatic method of segmentation of the kidney external surface in US images. The main objectives of this task are to improve the common measurements of the renal volume and the visualization and analysis of the organ shape. In the manual part the practitioner inserts six points that correspond to the main axes of the best-fit ellipsoid for the kidney surface [20]. This simple insertion is extended to those cases in which the whole kidney volume is not acquired, where the user must introduce twelve points that correspond, to the main axes of the visually estimated fit of an ellipse to the extremal and central kidney slice contours.

The automatic method is a model based segmentation one. It is a 3D extension of the method in [21]. It takes the points and builds an ellipsoid. Then it discretizes this surface by means of a cylindrical coordinate system induced parametrization. So the initial surface is described by a set of  $S = P \times J$  points that correspond respectively to the set of cuts and rays of the model. This template surface is refined by allowing its deformation into a discrete space defined by the set  $\Omega = \Lambda \times S$ , where  $\Lambda$  refers to a set of possible radial deformations in the surroundings of the template surface.

Each of the elements in  $\Omega$  define two regions in the volume image, namely a region of closeness and an inner region. The algorithm is going to construct the two external potential terms with the pixels included in these two regions. In our framework these terms contribute to the *a posteriori* likelihood terms. They are based respectively on an exponential distribution modeling of the image gradient and a beta distribution modeling of the image intensity. On the other side, from the locations of the possible deformation points and their neighbors, we can construct a predefined *a priori* model or the internal energy of the model that tries to maintain the smoothness of the surface by favoring those solutions in which the first and second finite radial deformation derivatives are small. Both trends are joined together into a Markov Random Field of deformations. The estimation of the relative importance of each of them as well as the estimation of the deformed surface are integrated in a Maximum a Posteriori framework [22, 23].

A result of a segmented contour in one slice of a healthy kidney is shown in figure 10. The code of the module is based on VTK and it is integrated with the rest of the functionalities in

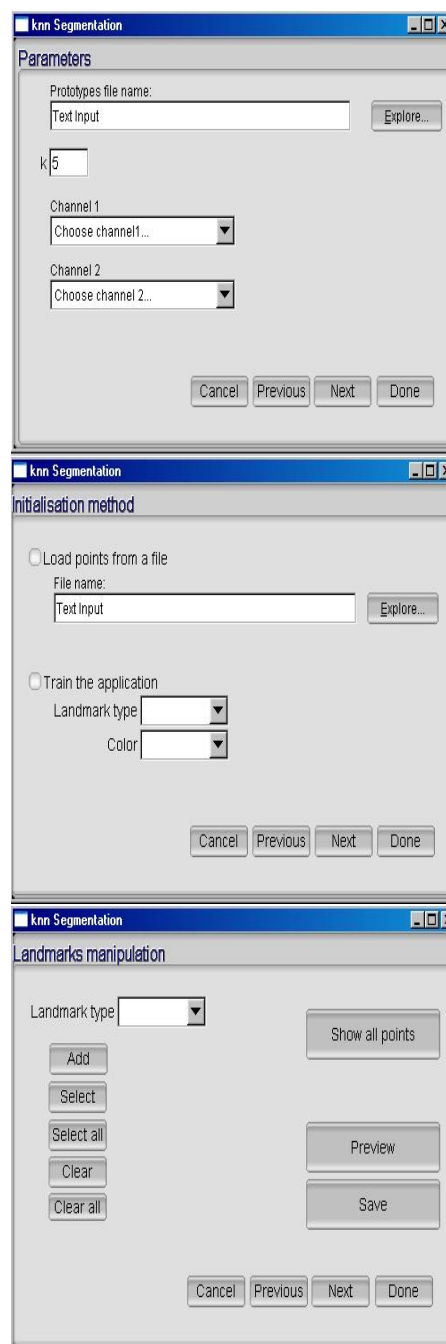


Figure 8: Wizard windows

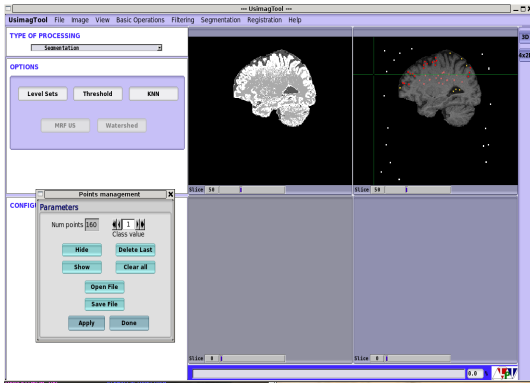


Figure 9: *kNN Segmentation in UsimagTool*

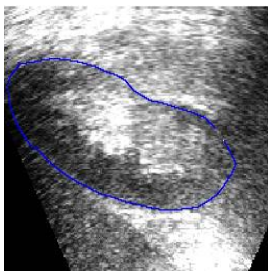


Figure 10: *2D kidney segmentation*

*UsimagTool*, although it is at this time a beta version. It seems clear for us that the method could be adapted for the segmentation of another abdominal organs as the liver or the prostate as pointed out in [21]. This could be interesting for taking a better advantage in the visual interpretation of 3D images acquired with modern echographic techniques.

### 3.3. Registration for Elastography

The Demons ITK algorithm has been added to the tool with general purpose. This workpackage is very important for the elastography intended part of *UsimagTool*, therefore own software has been implemented and modified to be adapted for elastography purposes as this modality has its specific needs. In this section, a brief description of elastography and the registration method used is described. This filter is in process to be added to the *UsimagTool*. This process will be finished after the eINTERFACE due to its difficult integration as it is not an ITK filter but a C++ module that needs to be compiled together with the main code.

Changes in tissue stiffness correlate with pathological phenomena that can aid the diagnosis of several diseases such as breast and prostate cancer. US elastography measures the elastic properties of soft tissues using US signals.

The standard way to estimate the displacement field from which researchers obtain the strain in elastography is the time-domain cross-correlation estimator (TDE). Optical flow (OF) methods have been also characterized and their use keeps increasing.

We have introduced the use of a modified demons algorithm (MDA) to estimate the displacement field. A least-squares strain estimator (LSE) is applied to estimate the strain from the displacement. The input for the algorithm comes from the US scanner standard video output; therefore, its clinical implementation is immediate. The resulting elastogram and the isochoic input precompression image for the simulated phantom are presented

in Figure 11. It is observed how an inclusion 3 times stiffer than the background can not be appreciated in the B-mode image of the experiment presented. However, at the elastogram, at the right of the same figure, the inclusion is clearly visible.

Although other researchers have used registration methods for elastography, as far as we know, it have not been used as stand alone but together with elastic modulus reconstruction or FE which iteratively varies material properties to improve registration. Our method does not requires any assumption about the isotropy or initialization for the algorithm, reducing the computational cost with respect to the other registration methods used for elastography. Compared to OF methods, we obtain a more regularized displacement field reducing the artifacts in the strain image. The advantage of these method based on the B-mode ultrasound image compared to those based on the RF A-lines (TDE) is the flexibility to include into commercial US scanner because the formerinput comes from the standard video output of the equipments. Decorrelation effects, mainly when dealing with pronounced strains, compromises the accuracy of the TDE methods. The obtained results have been already sent for its presentation in an international congress.

### 3.4. Filtering

Several classic filtering methods have been implemented in *UsimagTool* such as Gaussian, median, Wiener, or anisotropic filters, as well as a set of edge-detection techniques. Additionally we have developed new specific filters for US images: a Speckle Reducing Anisotropic filter (SRAD) [24], Detail Preserving Anisotropic Diffusion (DPAD) filter for speckle [25], a Tensor guided Anisotropic Diffusion filter (TAD) based on [26] and an anisotropic Wiener filter for speckle removal based on [22].

#### 3.4.1. Classic filtering methods

The following well-known methods has been included in the current *UsimagTool* version:

- Gaussian filtering: smoothing through a convolution with a Gaussian kernel of variance  $\sigma^2$ .
- Median filtering: block-wise median filtering [27].
- Mean filtering: sample average in a neighborhood.
- Wiener filter: Classic implementation of the Wiener filter; i.e. the Linear Minimum Mean Squared Error (LMMSE) estimator assuming Gaussian additive noise [27].
- Anisotropic Diffusion filtering schemes [28, 29, 30, 26].
- Edge-detection techniques: Zero crossing edge detector and Canny filter [27].

#### 3.4.2. Speckle Reducing Anisotropic Diffusion (SRAD) and Detail Preserving Anisotropic Diffusion (DPAD)

Anisotropic diffusion is a well known and widely used technique in image processing, since it offers a good compromise between noise removal and edge preservation; the original formulation by Perona and Malik [28] was based on the heat diffusion equation, where the gray level of the image,  $I$ , acts as the temperature that drives the heat conduction over the image.

This approach has shown a very good performance when dealing with additive noise. However, it seems to fail when working with US imaging, where the additive model does not hold. We use here the ideas proposed in [24], substituting this gradient-driven diffusion coefficient with a coefficient based on adaptive filtering theory; the coefficient of variation used in the LMMSE filtering for speckle removal [31, 32] is casted into the

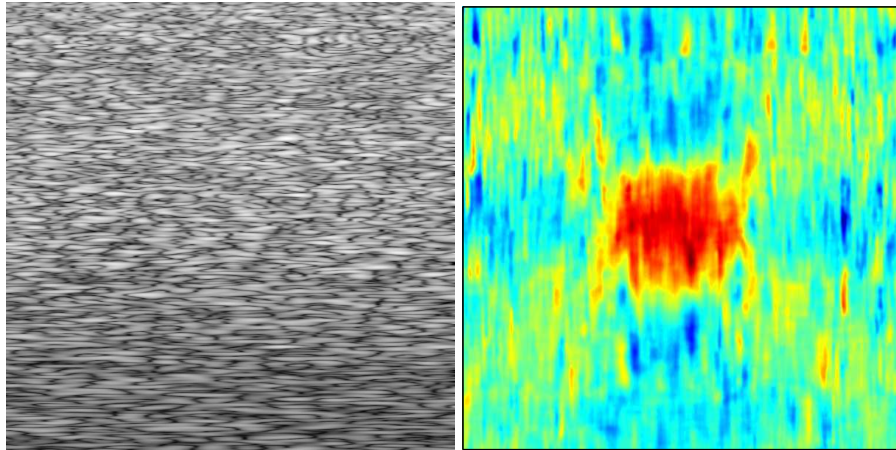


Figure 11: **Left:** Precompression B-mode image. **Right:** Strain image resulting from the MDA registration.

PDE environment, achieving a similar formulation to the original anisotropic one, but with the ability to cope with multiplicative noise.

Although the formulation of SRAD is deduced in [24] only for the 2D case, we have extended it to a 3D case. Moreover, given the templated nature of the ITK software, the same source code, with no modifications, is valid for both the 2D and 3D scenarios.

In [25] authors propose a more robust way to estimate the coefficient of variation in a SRAD scheme. This, together with a more complete solution produces an alternative scheme called Detail Preserving Anisotropic Diffusion (DPAD) filter. A new ITK class has been developed and included into *UsimagTool*.

### 3.4.3. Tensor Guided Anisotropic Diffusion Filtering (TAD)

One of the main issues with anisotropic diffusion filtering is the numeric scheme used to solve the PDE. The most usual way is the explicit implementation by means of finite differences: at a given iteration, the right hand side of the equation is computed given the current estimates of  $I(x, y, t)$ , and then the partial derivative in time is approximated by  $\partial I / \partial t \simeq (I(x, y, t + \tau) - I(x, y, t)) / \tau$  so that  $I(x, y, t + \tau)$  can be easily found by forward differences as:

$$I(x, y, t + \tau) = I(x, y, t) + \tau \nabla \cdot (c(I(x, y, t)) \cdot \nabla I(x, y, t)) \quad (1)$$

The problem with this scheme is that it needs a very low value of  $\tau$  (typically  $\tau < 1/4$  in the 2D case) for the system to be stable, so many iterations are needed to converge to the steady state. The solution given in [26] is to use a semi-implicit scheme, which has been proved to unconditionally converge for any value of  $\tau$ .

The method is said to be semi-implicit because one uses the gradient in the next time sample but the diffusion coefficient is assumed to be the one computed in the current iteration. Each step of the algorithm requires to solve a linear system of equations which is highly sparse, so a recursive algorithm may do this task with low computational cost [26].

On the other hand, traditional anisotropic diffusion is based on the fact that diffusion is simply stopped near relevant structures, so edges are preserved, but not enhanced. The approach of [33] generalizes the heat diffusion equation by the introduction of a diffusion tensor instead of the diffusion parameter, so  $c(x)$

is a  $2 \times 2$  matrix (in the 2D case); the eigenvectors of this matrix are set to be the same as those of the structure matrix of the image at this point. Regarding the eigenvalues, the one corresponding to the direction parallel to the contour is kept constant, meanwhile the eigenvalue along the orthogonal direction is also computed.

This way, near edge pixels there still exists a diffusion process, but it happens in a direction parallel to the contour. Far from the edges, the diffusion is isotropic to favor noise removal. This kind of filters not only preserve the contours, but they are able to enhance them as well. A semi-implicit implementation is derived once again to obtain an adequate computational behavior.

Although the work in [33] is intended for speckle removal, the problem is the same as in the case of scalar anisotropic diffusion: speckle is a multiplicative noise, so the additive model cannot be assumed. For this reason, we have adapted the algorithm to overcome the problem in a similar way to that introduced in [24] for the scalar case. The diffusion tensor is here computed based on local statistics specific for the US imaging case. The direction of the eigenvector parallel to the contour is found using the sticks model proposed by Czerwinski [34].

For the eigenvalues, a simple speckle classifier [35, 22] based on the moments of the homodyned  $k$ -distribution is used to discriminate fully formed speckle, where the diffusion is purely isotropic, and resolved speckle, where the diffusion is driven only following the sticks direction, which are ideally parallel to the contours of the US image.

### 3.4.4. Anisotropic Wiener Filter with Bias Correction

The Wiener filter, that is, the optimum linear filter in the minimum mean square error (LMMSE) allows to estimate a signal  $\mathbf{X}$  from its noisy observation  $\mathbf{Y} = \mathbf{X} + \mathbf{N}$ , where  $N$  is the additive noise [27]. Wiener filter is known to be optimal under the assumption of Gaussian distributed data. However, this assumption is not valid for US images, that are better modeled by a Rice distribution [36]. For this reason, the direct application of Wiener filtering would introduce a bias in the results. Therefore, our Wiener filter implementation includes a previous bias correction step based on the Rice distribution. It is based on the fact that the SNR (Signal to Noise Ratio) for a Rice distribution is a monotonic function that depends only on one parameter  $\gamma = \frac{S}{\sigma}$  [22], where  $S$  is the signal envelope and  $\sigma$  its variance. The SNR can be estimated from the observation by the method of the mo-

ments. Since the SNR function is monotonic, we can estimate the parameter  $\gamma$  from the estimated SNR value by means of the inverse function. On the other hand, the second order moment of the Rice distribution is given by  $EY^2 = 2\sigma^2 + s^2 = s^2 \frac{2+\gamma^2}{\gamma^2}$ . Therefore, the signal envelope can be estimated by the eq. (2).

$$\bar{s} = \sqrt{\frac{\bar{Y}^2 \gamma^2}{2 + \gamma^2}} \quad (2)$$

In such a way, we compute the bias corrected signal  $Y'(n) = Y(n) - \bar{Y}(n) + \bar{s}(n)$  and the anisotropic Wiener filtering is applied over it. The resulting approach eliminates the bias, maintains the underlying signal structure unaltered and at the same time reduces the local variability palliating the speckle effect.

#### 4. FUTURE OF USIMAGTOOL

Although *UsimagTool* is now in an advance stage, there is still too many work to do. We need to complete some of the tasks in the immediate future such as: integration of the elastography algorithms and other filtering algorithms developed during eNTERFACE 07, addition of vector image processing, complete the on-line help and the user and developers manual, and redesign some of the features of the GUI in order to make them more intuitive and easy to use. Another immediate task is the integration and testing of the wiimote control, in order to improve the interaction with the user.

Additionally we plan to restructure part of the main classes of the code to make it even more modular than now, and therefore more easy for a new user to include new functionalities. In the long term, we will include tensor data support: input and output using the tensor standard developed in similar, and also processing and visualization capabilities.

#### 5. CONCLUSIONS

We can say that the work done in eNTERFACE 07, has been quite useful for the development of a new graphical user interface designed to help researchers in the development and use of algorithms for US image processing, that can be also used for other image modalities. The features of this tool makes it quite useful for researchers, due to the flexibility offered by its simple architecture, that allows to include new algorithms very fast. It is also important to highlight that this is an open source project which is available on line in <http://www.lpi.tel.uva.es/usimagtool>.

The work done in the redesign of the interface has been intensive from the whole eNTERFACE period, and the final result although not finished is quite satisfactory. We have improve the 3D viewer for surface rendering, and we improve the 2D viewers in order to include support for points management.

We have also developed some algorithms for US elastography although they are not included in *UsimagTool*. We have also implemented several algorithms not included in the official ITK release: one supervised segmentation method (kNN), one segmentation algorithm for US kidney based a MRF model, and the filtering algorithms: TAD, DPAD and SRAD, they all based on well known published works. We have also included in this tool many other well known algorithms from the ITK official release that are very useful for developers.

In order to improve interaction with the user we have studied the Wiimote control which provides many capabilities to the user and that we consider quite interesting also because it is a low cost device. We have developed a simple interaction mode with this device in a prototype with successful results, but more work is still needed.

We have also taken especial care in the multi-platform compatibility (windows and linux), so the same source code can be compiled and executed in both operating systems.

We can state that with all these accomplished tasks, the work done for *UsimagTool* has been quite satisfactory. We began with a prototype in a very early stage of development and now we can say that this tool has the features of an advanced software package for US image processing.

#### 6. ACKNOWLEDGEMENTS

This work have been funded by CEE SIMILAR NoE (FP6-5076-09) and Spanish Government Project USIMAG (TEC2004-06647-C03-02).

#### 7. REFERENCES

- [1] L. Ibañez, W. Schroeder, L. Ng, and J. Cates, *The ITK Software Guide*. Kitware, Inc., second ed., 2005. ISBN 1-930934-15-7. <http://www.itk.org/ItkSoftwareGuide.pdf>. 117
- [2] W. Schroeder, K. Martin, and W. Lorensen, *The Visualization Toolkit: An Object Oriented Approach to Computer Graphics*. Kitware, Inc, third ed., 2004. <http://www.vtk.org>. 117
- [3] I. Wolf, M. Vetter, I. Wegner, T. Böttger, M. Nolden, M. Schöbinger, M. Hastenteufel, T. Kunert, and H. Meinzer, "The Medical Imaging Interaction Toolkit", *Medical Image Analysis*, vol. 9, pp. 594–604, 2005. 117
- [4] MIT Artificial Intelligence Lab and the Surgical Planning Lab at Brigham & Women's Hospital, Harvard Medical School, *3D Slicer. 3D Slicer software*. <http://www.slicer.org>. 117
- [5] D. Gering, A. Nabavi, R. Kikinis, W. E. L. Grimson, N. Hata, P. Everett, F. Jolesz, and W. W. III, "An Integrated Visualization System for Surgical Planning and Guidance using Fusion and Interventional Imaging", in *MICCAI*, (Cambridge, England), pp. 808–819, Sept 1999. 117
- [6] Research center caesar, Bonn, Germany, *The Julius software platform*. <http://www.julius.caesar.de>. 117
- [7] A. Rosset, L. Spadola, and O. Ratib, "OsiriX: An Open-Source Software for Navigating in Multidimensional DICOM Images", *J Digit Imaging*, vol. 17, pp. 205–216, Sep 2004. 117
- [8] P. Yushkevich, J. Piven, H. Hazlett, R. Smith, S. Ho, J. Gee, and G. Gerig, "User-Guided 3D Active Contour Segmentation of Anatomical Structures: Significantly Improved Efficiency and Reliability", *Neuroimage*, vol. 31, no. 3, pp. 1116–1128, 2006. 117
- [9] V. Nicolas, UCL, *MedicalStudio*. <http://www.medicalstudio.org>. 117
- [10] P. Fillard, N. Toussaint, and X. Pennec, "MedINRIA: DT-MRI Processing and Visualization Software", November 2006. Guest paper at the Similar Tensor Workshop, Las Palmas, Spain. 117
- [11] A. Loening and S. Gambhir, "AMIDE: a free software tool for multimodality medical image analysis", *Molecular Imaging*, vol. 2, no. 3, pp. 131–137, 2003. 117
- [12] Y. Lu, S. Pathak, L. Gong, J. Goldschneider, and P. Kinahan, "Open Source Medical Image Fusion Display". <http://fusionviewer.sourceforge.net>. 117

- [13] Mayo Clinic, *ANALYZE software*. <http://www.mayo.edu/bir/Software/Analyze/Analyze.html>. 117
- [14] Mercury Computer Systems Inc., *Amira*. <http://www.amiravis.com>. 117
- [15] Able Software Corp., *3D Doctor*. <http://www.ablesw.com/3d-doctor>. 117
- [16] “C Wiimote Library”. <http://www.wiimote.net>. 120
- [17] S. Warfield, “Fast k-NN Classification for Multichannel Image Data”, *Pattern Recognition Letters*, vol. 17(7), pp. 713–721, 1996. 121
- [18] O. Cuisenaire and B. Macq, “Fast k-NN Classification with an Optimal k-Distance Transformation Algorithm”, *Proc. 10th European Signal Processing Conf.*, pp. 1365–1368, 2000. 121
- [19] R. Cárdenes, M. R. Sánchez, and J. Ruiz-Alzola, “Computational Geometry Computation and KNN Segmentation in ITK”, *Insight Journal, ISC/NA-MIC Workshop on Open Science at MICCAI 2006*, Oct 2006. <http://hdl.handle.net/1926/204>. 121
- [20] J. Bakker, M. Olree, R. Kaatee, E. de Lange, K. Moons, J. Beutler, and F. J. Beek, “Renal volume measurements: accuracy and repeatability of US compared with that of MR imaging”, *Radiology*, vol. 211, pp. 623–628, 1999. 121
- [21] M. Martin and C. Alberola, “An approach for contour detection of human kidneys from ultrasound images using Markov random fields and active contours”, *Medical Image Analysis*, vol. 9, no. 1, pp. 1–23, 2005. 121, 122
- [22] M. Martin-Fernandez, E. Muñoz-Moreno, and C. Alberola-Lopez, “A Speckle Removal Filter based on an Anisotropic Wiener Filter and the Rice Distribution”, in *IEEE International Ultrasonics Symposium*, (Vancouver, Canada), pp. 1694–1697, Oct 2006. 121, 122, 123
- [23] S. Lakshmanan and H. Derin, “Simultaneous parameter estimation and segmentation of Gibbs Random Fields using Simulated Annealing”, *IEEE Transactions on Pattern Analysis and Machine Intelligence*, vol. 11, pp. 799–813, Aug. 1989. 121
- [24] Y. Yongjian and S. Acton, “Speckle reducing anisotropic diffusion”, *IEEE Transactions on Image Processing*, vol. 11, pp. 1260–1270, Nov 2002. 122, 123
- [25] S. Aja-Fernandez and C. Alberola-Lopez, “On the Estimation of the Coefficient of Variation for Anisotropic Diffusion Speckle Filtering”, *IEEE Transactions on Image Processing*, vol. 15, no. 9, pp. 2694–2701, 2006. 122, 123
- [26] J. Weickert, B. ter Haar Romeny, and M. Viergever, “Efficient and reliable schemes for nonlinear diffusion filtering”, *IEEE Transactions on Image Processing*, vol. 7, pp. 398–410, Mar. 1998. 122, 123
- [27] J. Lim, *Two Dimensional Signal and Image Processing*. Prentice Hall, 1990. 122, 123
- [28] J. M. P. Perona, “Scale-space and edge detection using anisotropic diffusion”, *PAMI*, vol. 12, pp. 629–639, July 1990. 122
- [29] R. K. G. Gerig, O. Käbler and F. Jolesz, “Nonlinear anisotropic filtering of MRI data”, *IEEE Transactions on Medical Imaging*, vol. 11, pp. 221–232, June 1992. 122
- [30] F. Catté, P. Lions, J. Morel, and T. Coll, “Image selective smoothing and edge detection by nonlinear diffusion”, *SIAM J. Numer. Anal.*, vol. 29, pp. 182–193, 1992. 122
- [31] J. S. Lee, “Digital image enhancement and noise filtering by using local statistics”, *IEEE Trans. on Pattern Analysis and Machine Intelligence*, vol. 2, no. 1, 1980. 122
- [32] V. S. Frost, J. A. Stiles, K. S. Shanmugan, and J. C. Holtzman, “A model for radar images and its application to adaptive filtering of multiplicative noise”, *IEEE Trans. on Pattern Analysis and Machine Intelligence*, vol. 4, no. 1, pp. 157–165, 1982. 122
- [33] K. Z. Abd-Elmoniem, A. M. Youssef, and Y. M. Kadah, “Real-Time Speckle Reduction and Coherence Enhancement in Ultrasound Imaging via Nonlinear Anisotropic Diffusion”, *IEEE Trans. on Biomedical Engineering*, vol. 49, no. 9, pp. 997–1014, 2002. 123
- [34] R. N. Czerwinski, D. L. Jones, and W. J. O’Brien, “Line and Boundary Detection in Speckle Images”, *IEEE Trans. on Image Processing*, vol. 7, no. 12, pp. 1700–1714, 1998. 123
- [35] R. W. Prager, A. H. Gee, G. M. Treece, and L. H. Berman, “Decompression and speckle detection for ultrasound images using the homodyned k-distribution”, *Pattern Recognition Letters*, vol. 24, pp. 705–713, 2003. 123
- [36] T. A. Tuthill, R. H. Sperry, and K. J. Parker, “Deviation from Rayleigh Statistics in Ultrasonic Speckle”, *Ultrasonic Imaging*, vol. 10, pp. 81–89, 1988. 123

## 8. BIOGRAPHIES



**Rubén Cárdenes-Almeida** received his M.S. degree in physics from the University of Zaragoza in 1998, and he received his PhD degree in 2004 from the University of Las Palmas de Gran Canaria (ULPGC), at the Telecommunication Engineering School. He has been teaching and working in several research projects in the Center for Technology in Medicine (CTM), at the ULPGC, and he is currently working as a postdoc in the University of Valladolid, in the Laboratory of Image Processing (LPI), where he participates in various national and international research projects since March 2006. From June 2000 he also collaborates with the Surgical Planning Lab (SPL), at Brigham & Women’s Hospital, (Harvard Medical School), where he has been invited researcher several times. His PhD thesis and current research work are related to medical image processing and discrete computational geometry.

Email: [ruben@lpi.tel.uva.es](mailto:ruben@lpi.tel.uva.es)



**Antonio Tristán-Vega** received his M.E. degree on Telecommunications engineering in 2004, at the University of Valladolid. He is currently a PHD student at this same University, and participates in a number of national and regional research projects as a member of the Laboratory of Image Processing (LPI). His research interests comprise multimodal and interpatient image fusion, image registration, and computer aided diagnosis based on medical imaging.

Email: [atrive@lpi.tel.uva.es](mailto:atrive@lpi.tel.uva.es)



**Gonzalo Vegas-Sánchez-Ferrero** is a PhD student at University of Valladolid, Spain. He received his Engineering of Telecommunication degree from that university in October 2006. He is a research affiliate at the Laboratory of Image Processing (LPI), Valladolid, Spain. Currently is working in tensor field processing in resonance imaging of the left-ventricular endocardium and epicardium

of the heart.

Email: [gvegsan@lpi.tel.uva.es](mailto:gvegsan@lpi.tel.uva.es)



**Rodrigo de Luis-García** graduated in Telecommunications Engineering from the University of Valladolid in 2002, and received his PhD degree in Signal Processing at the Laboratory of Image Processing (LPI) from the same university in 2007. Most of his research activity focuses on the development of novel segmentation techniques for Medical Imaging applications. His work has been published in several international journals and conferences. Currently, he is an assistant professor at the Department of Signal Processing and Communications of the University in Valladolid, and has been recently awarded with a postdoctoral Fulbright scholarship.

Email: [rluigar@lpi.tel.uva.es](mailto:rluigar@lpi.tel.uva.es)



**Santiago Aja-Fernández** is currently an Assistant Professor with the ETSI Telecomunicación, the University of Valladolid, and is also with the Laboratory of Image Processing (LPI) at the same university. He received the Engineering of Telecommunication and Ph.D. degrees, both from the University of Valladolid, Valladolid, Spain, in 1999 and 2003 respectively. His research interests are fuzzy techniques for

image and signal processing. In 2006 he was been awarded with a Fulbright Scholarship for a one year stay as a Research Fellow in the Laboratory of Mathematics in Imaging at Brigham and Women's Hospital (Boston).

Email: [sanaja@tel.uva.es](mailto:sanaja@tel.uva.es)



**Javier González-Fernández** received the Degree in Industrial Engineering in 2000 from the University of Las Palmas de Gran Canaria (ULPGC), Spain. He is now a PhD candidate at the Center for Technology in Medicine, ULPGC. His research interests include Ultrasound Elastography, hardware design for biomedical embedded systems, and DSP.

Email: [jgonzalez@ctm.ulpgc.es](mailto:jgonzalez@ctm.ulpgc.es)



**Verónica García-Pérez** received her Master Engineering in Computing Science degree from the Computer Science School, at the University of Valladolid, Spain, in 2004. Currently, she is PhD student in the Telecommunications School, in the signal processing area, where she also participates in a number of national and international research projects. She is a research

fellow in the Laboratory of Image Processing (LPI) at this same University. Her main research interests comprise fuzzy systems, virtual reality and surgical simulation.

Email: [veronica@lpi.tel.uva.es](mailto:veronica@lpi.tel.uva.es)



**Darío Sosa-Cabrera** received the Mechanical Engineer degree from the University of Las Palmas de Gran Canaria (2001), is currently a PhD student in the Telecommunications Engineering School, focusing on US Elastography. He has studied in France at IFMA. After working in Latvia, he has coursed a Management of Technology Master at UTSA and joined the Department of Radiology, University of

Texas, Houston, for one semester.

Email: [dario@ctm.ulpgc.es](mailto:dario@ctm.ulpgc.es)



**Emma Muñoz-Moreno** received her M.S. degree in Electronical Engineering from the University of Valladolid in 2003, and currently she is a PhD student at the same received University. She has participated in several national and international research projects as member of the Image Processing Laboratory at the University of

Valladolid. Her research work is related to medical image processing, specially registration algorithms of DT-MRI and surgical simulation.

Email: [emunmor@lpi.tel.uva.es](mailto:emunmor@lpi.tel.uva.es)



**Karl Krissian** received his M.S. in computer science and artificial intelligence from the university of Paris XI and the Ecole Normale Supérieure de Cachan in 1996. He received his Ph.D. degree in Computer Vision from the university of Nice-Sophia Antipolis and the INRIA in 2000. His main research topics are filtering and segmentation of three-dimensional vascular images using Partial Derivative Equations. He is currently working at the university of Las Palmas of Gran Canaria in Spain.

Email: [krissian@dis.ulpgc.es](mailto:krissian@dis.ulpgc.es)



**Suzanne Kieffer** was born in Thionville, France, in 1977. She graduated in Computer Science at the University of Metz, France, in 1998 and she obtained MPhil in Computer Science in 2001. She defended her PhD thesis entitled “Multimodal assistance in the visual exploration of 2D interactive visualisations” in 2005 at the Université Henri Poincaré of Nancy, France.

At the present time she is post-doctoral researcher at the Université Catholique de Louvain at the Communication and Remote Sensing Laboratory (TELE) and she is also member of the Belgium Computer-Human Interaction Laboratory (BCHI). Her research topics are focused on Human-Computer Interaction (HCI). In particular, they are related to Ergonomics, Graphical User Interfaces (GUI), Interaction Techniques and Usability Evaluation of Multimodal Interfaces.

Email: [suzanne.kieffer@uclouvain.be](mailto:suzanne.kieffer@uclouvain.be)